Density Functional Theory Study of the Structures and Stabilities of CuO_3^- and CuO_3

ZEXING CAO,[1] MIQUEL SOLÀ,[2] HUI XIAN,[1] MIQUEL DURAN,[2] QIANER ZHANG[1]

[1]*Department of Chemistry, State Key Laboratory for Physical Chemistry of the Solid Surface and Institute of Physical Chemistry, Xiamen University, Xiamen 361005, People's Republic of China*
[2]*Institute of Computational Chemistry and Department of Chemistry, Universitat de Girona, 17071 Girona, Catalonia, Spain*

Received 14 April 2000; revised 7 June 2000; accepted 20 July 2000

ABSTRACT: Hybrid density functional theory calculations on the structures, vibrational frequencies, electron binding and dissociation energies, and bonding properties of CuO_3^- and CuO_3 species have been carried out. Stable isomers containing an O_3 subunit and composed of O_2 bound to CuO have been located on the potential energy hypersurfaces of CuO_3^- and CuO_3. The isomers formed by O_2 bonded to CuO in side-on and end-on coordination are more stable than those containing an O_3 subunit. © 2001 John Wiley & Sons, Inc. Int J Quantum Chem 81: 162–168, 2001

Key words: CuO_3^- and CuO_3; structure and bonding; vibrational frequencies; electron binding and dissociation energies; DFT calculations

Introduction

The interaction of transition metals with oxygen is of broad chemical and biochemical interest [1, 2]. Many theoretical and experimental studies have been directed at CuO and CuO_2 [3–8]. In a recent anion photoelectron spectroscopy study [9], a new CuO_3^- molecule was observed for the first time. CuO_3^- contains a CuO^- bonded to an O_2 molecule and dissociates at 3.49 eV into CuO^- and O_2. A minor isomer, $Cu(O_3)^-$, was also generated by the plasma reactions between the laser-vaporized copper atoms and O_2 [9]. The isomers of CuO_3 could be classified into two kinds. One is formed by O_2 bound to CuO, and the other is composed of Cu and an O_3 subunit (see Fig. 1). The structure and bonding features of these species are unknown. Thus, theoretical works on these $Cu/O/O_2$ species observed are necessary to better understand the

Correspondence to: M. Solà; e-mail: miqel@iqc.udg.es.
Contract grant sponsor: Spanish DGES.
Contract grant number: PB98-0457-C02-01.
Contract grant sponsor: China NSF.
Contract grant number: 29773036.
Contract grant sponsor: Catalan Comissionat per a Universitats i Recerca.

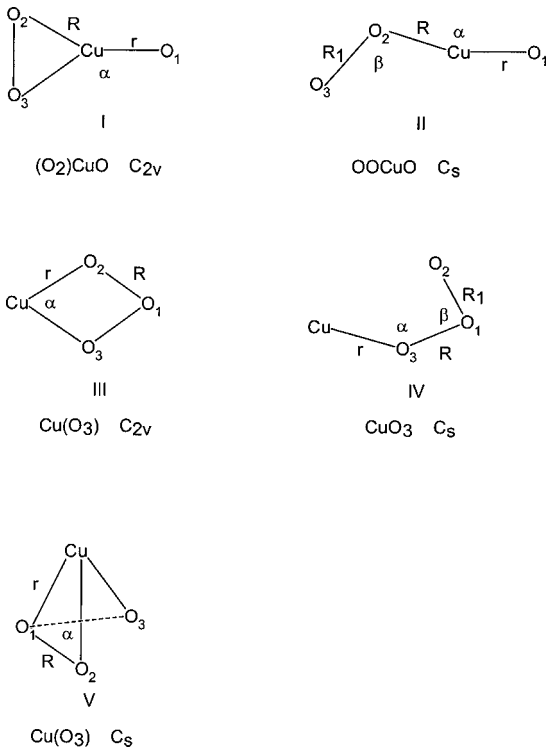

FIGURE 1. Schematic drawing with labels and geometrical parameters of the different CuO_3 isomers studied.

copper–oxygen chemical bonding, which is important in several areas of chemistry and biochemistry. To fulfill this goal we have carried out a density functional theory (DFT) study of CuO_3^- and CuO_3. The structures and vibrational frequencies of the low-lying states for the CuO_3^- and CuO_3 species have been calculated. The dissociation behavior and the photoelectron spectra for the stable CuO_3^- isomers have been discussed.

Computational Details

DFT has become increasingly popular in the last decade for calculating transition-metal compounds because the gradient-corrected exchange and correlation functionals give results that have a comparable and frequently higher accuracy than ab initio calculations [10–17]. In particular, Barone and Adamo [11b] have found that the DFT methodology yields satisfactory results for CuO_2 species as compared to experiment and high-level post–Hartree–Fock approaches. Thus, DFT methodologies have been used in the present study to obtain the optimized geometries, energetics, and vibrational frequencies of CuO_3^- and CuO_3 species. In the DFT calculations, the Becke's three-parameter hybrid exchange functional [18] has been combined with the Perdew's gradient-corrected correlation functional [19] (B3P86) and the Lee–Yang–Parr's nonlocal correlation functional [20] (B3LYP). The default fine-grid implemented in the Gaussian 94 program [21] has been used throughout. Single and double substitutions with noninterative triple excitations coupled cluster [CCSD(T)] [22] energy calculations for the lowest-lying states of CuO_3^- and CuO_3 have been carried out at the optimized B3P86 geometries (CCSD(T)//B3P86) to confirm the validity of DFT relative energies. At the DFT level, natural bond orbital (NBO) analyses [23] on relevant states have been performed to discuss the characteristics of metal–ligand interactions. This method allows to quantitatively describe the electronic state of the partners in a complex and to isolate donation and backdonation contributions to metal–ligand interactions.

The basis set used for all atoms has been the 6-311+G*, which, for copper, is the all-electron basis set by Wachters and Hay [24, 25] with the scaling factor of Raghavachari and Trucks [26]. An *f* polarization function and a set of *s*, 2*p*, and *d*-type diffuse functions for copper have been included. We have found that the inclusion of a *g*-type polarization function for copper has a minor effect on the geometry of the ground state of CuO_3^-.

Results and Discussion

Equilibrium geometries, electron configurations, S^2, relative energies, vibrational frequencies, and corresponding intensities of the lowest-lying states of CuO_3^- and CuO_3 species obtained at the B3P86 level are collected in Table I. Stable species listed in Table I were also optimized with the B3LYP method. The B3LYP results are not included in this table because the differences found between the B3P86 and B3LYP geometries were in all cases very small. Table II presents approximated electron binding energies, while Table III lists dissociation energies of stable CuO_3^- isomers. Natural population analysis and natural valence electron configurations for several selected states are shown in Table IV.

For CuO_3^-, among the states of C_{2v} (I) isomer located by the B3P86 and B3LYP methods, only the singlet $^1A_1$ state is stable, while all triplet states are transition states leading to the C_s (II) isomer, an end-

on structure in which O_2 is bound to CuO. In a previous theoretical study of CuO_2 by Barone and Adamo [11b], the end-on structure was also found to be more stable than the side-on structure. Following the imaginary mode of the $^3B_1$ triplet state of C_{2v} (I) structure, we have found a stable $^3A''$ state of C_s (II) structure, lower in energy than the $^3B_1$ state by 3.4 and 2.4 kcal/mol at the B3LYP and B3P86 levels of theory, respectively. This $^3A''$ state of C_s (II) symmetry is the ground state of CuO_3^-. It is more stable than the $^1A_1$ state of C_{2v} (II) symmetry by 9.9, 12.3, and 1.0 kcal mol^{-1} at the B3P86, B3LYP, and

TABLE I

Electronic configurations, geometries, harmonic vibrational frequencies, intensities, S^2 values, and relative energies calculated at the DFT/B3P86 level.

State	Configuration[a]	Geometry[b]	Frequencies[c]	$\langle S^2 \rangle$	RE[d]
CuO_3^- anion					
$(O_2)CuO\ C_{2v}$ (I)					
$^1A_1$	$7a_1^2\ 3b_2^2\ 3b_1^2\ 2a_2^2$	1.681, 1.845 158.0	136(19), 219(25), 479(0) 499(4), 826(43), 1034(258)	0.0	9.9 (10.6)
$^3B_1$	$7a_1^2\ 3b_2^2\ 3b_1^2\ a_2^2$ $b_2\ a_2$	1.723, 2.039 161.0	160*i*(4), 151(11), 165(20) 345(40), 697(9), 1184(115)	2.02	2.4 (2.2)
$^3A_2$	$7a_1^2\ 3b_2^2\ 3b_1^2\ 2a_2^2$ $b_2\ b_1$	1.754, 1.930 158.7	80*i*(25), 156(29), 213(1) 356(4), 612(3), 1005(83)	2.02	5.8 (5.3)
$OOCuO\ C_s$ (II)					
$^3A''$	$10a'^2\ 4a''^2\ a'\ a''$	1.749, 1.871 1.330, 175.4 112.0	107(13), 154(38), 174(17) 459(2), 626(8), 1193(11)	2.01	0.0 (0.0)
$Cu(O_3)\ C_{2v}$ (III)					
$^1A_1$	$6a_1^2\ 4b_2^2\ 3b_1^2\ 2a_2^2$	1.950, 1.448 73.8	247*i*(25), 350(36), 360(5) 647(7), 745(51), 882(21)	0.0	41.0 (41.4)
$^3B_2$	$6a_1^2\ 3b_2^2\ 3b_1^2\ 2a_2^2$ $b_2\ a_1$	1.896, 1.442 71.7	162(1), 367(9), 416(16) 663(50), 791(4), 935(1)	2.01	54.2 (55.1)
$^3B_1$	$6a_1^2\ 4b_2^2\ 2b_1^2\ 2a_2^2$ $b_1\ a_1$	2.196, 1.338 60.4	104*i*(3), 213(26), 243(0) 689(8), 911(139), 1073(22)	2.01	42.0 (42.6)
$CuO_3\ C_s$ (IV)					
$^3A''$	$10a'^2\ 4a''^2\ a'\ a''$	1.963, 1.378 1.303, 114.9 114.5	80(5), 186(1), 320(24) 650(5), 851(191), 1135(84)	2.01	41.3 (42.0)
$Cu(O_3)\ C_s$ (V)					
$^1A'$	$9a'^2\ 6a''^2$	2.388, 1.422 107.5	237(47), 294(6), 299(7) 648(19), 797(47), 875(344)	0.0	39.5 (40.1)
CuO_3 neutral					
$(O_2)CuO\ C_{2v}$ (I)					
$^2A_2$	$7a_1^2\ 3b_2^2\ 3b_1^2\ a_2^2$ a_2	1.665, 1.905 160.4	132(12), 196(15), 413(0) 436(3), 844(10), 1297(234)	0.76	21.5 (22.2)
$^2B_2$	$7a_1^2\ 2b_2^2\ 3b_1^2\ 2a_2^2$ b_2	1.783, 1.879 159.8	201*i*(42), 161(18), 331(2) 405(1), 635(42), 1236(152)	0.86	33.5 (33.4)
$^2B_1$	$7a_1^2\ 3b_2^2\ 2b_1^2\ 2a_2^2$ b_1	1.725, 1.864 159.2	116(13), 169(17), 386(1) 412(2), 689(16), 1156(259)	1.04	18.0 (18.1)
$^4A_1$	$7a_1^2\ 3b_2^2\ 2b_1^2\ a_2^2$ $b_2\ b_1\ a_2$	1.733, 1.958 160.9	123(11), 149(16), 277(0) 378(4), 674(17), 1261(333)	3.77	0.0 (0.0)

(Continued)

TABLE I
(Continued)

State	Configuration[a]	Geometry[b]	Frequencies[c]	$\langle S^2 \rangle$	RE[d]
$^4A_2$	$7a_1^2\ 2b_2^2\ 3b_1^2\ a_2^2$ $2b_2\ a_2$	1.812, 2.019 162.0	405*i*(64), 58(0), 123(15) 277(14), 584(0), 1393(157)	3.99	13.6 (13.0)
OOCuO C_s (II)					
$^4A''$	$9a'^2\ 4a''^2\ 2a'\ a''$	1.743, 1.829 1.231, 177.9 131.7	104(16), 108(9), 194(6) 402(26), 654(19), 1401(901)	3.77	3.8 (3.8)
$Cu(O_3)$ C_{2v} (III)					
$^2B_1$	$6a_1^2\ 4b_2^2\ 2b_1^2\ 2a_2^2$ b_1	2.040, 1.336 65.4	208(6), 260(10), 338(20) 744(1), 904(288), 1086(4)	0.75	7.0 (7.9)
$^2B_2$	$6a_1^2\ 3b_2^2\ 3b_1^2\ 2a_2^2$ b_2	1.844, 1.441 73.5	44(2), 344(2), 468(2) 707(9), 741(17), 958(0)	0.76	31.3 (30.3)

[a] Core electrons are omitted. Numbers in front of molecular orbitals indicate the number of orbitals with the same symmetry in the wavefunction.
[b] Geometry (Å, degrees): r, R, R_1, α, β, respectively, refer to Figure 1.
[c] Frequencies in cm^{-1}, intensities in parentheses in km mol^{-1}.
[d] Relative energies (kcal mol^{-1}) refer the $^3A''$ (II) and the $^4A_1$ state for CuO_3^- and CuO_3, respectively. Values in parentheses corrected by zero-point energies.

CCSD(T)//B3P86 levels of theory, respectively. For the species containing an O_3 subunit bound to Cu, the $^3B_2$ state of C_{2v} (III), the $^3A''$ state of C_s (IV), and the $^1A'$ state of C_s (V) are stable minima on the potential energy surface of CuO_3^-. The side-on singlet $^1A_1$ state of $Cu(O_3)^-$ (III) is a transition state that leads to the $^1A'$ state of the top-on $Cu(O_3)^-$ (V) during geometry optimization. The relative energy ordering predicted by B3P86 and B3LYP calculations for stable CuO_3^- isomers is as follows:

$$\begin{aligned} &OOCuO^-\ C_s\ (II) < (O_2)CuO^-\ C_{2v}\ (I) \\ &< Cu(O_3)^-\ C_s\ (V) \sim CuO_3^-\ C_s\ (IV) \\ &< Cu(O_3)^-\ C_{2v}\ (III). \end{aligned}$$

The isomers formed by O_2 bound to CuO are more stable than the species containing an O_3 subunit.

Note that the doublet and quartet states in C_{2v} (I), C_s (II), and C_{2v} (III) symmetry are stable for the neutral CuO_3 species. Among these stable states, the quartet $^4A_1$ state of $(O_2)CuO$ (I) is more stable than the $^2B_1$ (I) and $^4A''$ (II) states by 18.0 and 3.8 kcal mol^{-1} at the B3P86 level and by 18.2 and 3.0 kcal mol^{-1} at the B3LYP level, respectively. The $^4A_1$ (I) and $^4A''$ (II) states are very close in energy. Actually, while according to B3P86 and B3LYP results the ground state of neutral CuO_3 species is the $^4A_1$ (I) state, the CCSD(T)//B3P86 calculations

TABLE II
Electron binding energies (in eV) calculated at the B3LYP and B3P86 levels.

Ionization process	B3P86	B3LYP[a]	Experimental[b]
$^1A_1$ (I) $\longrightarrow$ $^2B_1$ (I)	3.67	3.13 (3.38)	3.39
$^3A''$ (II) $\longrightarrow$ $^4A''$ (II)	3.48	3.00 (3.25)	3.19
$^3A''$ (II) $\longrightarrow$ $^4A_1$ (I)	3.32	2.87 (3.54)[c]	
$^3B_2$ (III) $\longrightarrow$ $^2B_2$ (III)	2.23	1.84 (1.87)	
$^3A''$ (IV) $\longrightarrow$ $^2B_1$ (III) ($^2A''$ (IV))[d]	1.83	1.41 (1.73)	
$^1A'$ (V) $\longrightarrow$ $^2B_1$ (III) ($^2A'$ (V))[d]	1.90	1.85 (1.88)	

[a] Vertical ionization potentials in parentheses.
[b] Ref. [9].
[c] $^4A''$ (II) vertical electronic state.
[d] The vertical electronic states in parentheses, which decay to the $^2B_1$ (III) state during optimization process.

TABLE III
Dissociation energies of CuO_3^- calculated at the B3LYP and B3P86 levels.[a]

Dissociation process	B3LYP	B3P86[b]
$(O_2)CuO^-$ ($^1A_1$, I) $\longrightarrow$ O_2^- ($^2\Pi_g$) + CuO ($^2\Pi$)	58.8	64.0 (61.9)
$(O_2)CuO^-$ ($^1A_1$, I) $\longrightarrow$ O_2 ($^1\Delta_g$) + CuO^- ($^1\Sigma$)	75.6	79.7 (78.4)
$OOCuO^-$ ($^3A''$, II) $\longrightarrow$ O_2^- ($^2\Pi_g$) + CuO ($^2\Pi$)	71.1	73.9 (72.5)
$OOCuO^-$ ($^3A''$, II) $\longrightarrow$ O_2 ($^3\Sigma_g^-$) + CuO^- ($^1\Sigma$)	49.3	50.7 (50.1)
$Cu(O_3)^-$ ($^3B_2$, III) $\longrightarrow$ O_3^- ($^2B_1$) + Cu (^2S)	13.1	16.1 (14.9)
$Cu(O_3)^-$ ($^3B_2$, III) $\longrightarrow$ O_3 ($^1A_1$) + Cu^- (^1S)	48.4	51.7 (51.5)
CuO_3^- ($^3A''$, IV) $\longrightarrow$ O_3^- ($^2B_1$) + Cu (^2S)	26.7	29.1 (28.1)
CuO_3^- ($^3A''$, IV) $\longrightarrow$ O_3 ($^1A_1$) + Cu^- (^1S)	62.0	64.6 (64.7)
$Cu(O_3)^-$ ($^1A'$, V) $\longrightarrow$ O_3^- ($^2B_1$) + Cu (^2S)	28.4	30.8 (29.9)
$Cu(O_3)^-$ ($^1A'$, V) $\longrightarrow$ O_3 ($^1A_1$) + Cu^- (^1S)	63.8	66.3 (66.4)

[a] The dissociation energies are estimated by the difference: E(products) $-$ E(reactant), in kcal/mol.
[b] Values in parentheses have been corrected by zero-point vibrational energies.

yields the $^4A''$ (II) state as the ground state of the neutral CuO_3 species. At the CCSD(T)//B3P86 level of theory the $^4A''$ (II) state is more stable than the $^4A_1$ (I) state by 0.9 kcal mol^{-1}. No minima corresponding to the $Cu(O_3)$ (V) and CuO_3 (IV) isomers have been found in the potential energy surface. Starting from $Cu(O_3)$ (V) and CuO_3 (IV) structures, the optimization process leads invariably to the C_{2v} (III) structure.

In the most stable $^3A''$ state of the $OOCuO^-$ (II) species, the B3P86 calculation predicted a Cu–O stretching vibrational frequency of 626 cm^{-1}, which is lower by 91 cm^{-1} than the B3P86 calculated Cu–O stretching frequency in the CuO^- ($^1\Sigma$) system. For neutral isomers, the lowest $^4A_1$ state and the next lowest $^4A''$ state have Cu–O stretching vibrational frequencies of 674 and 635 cm^{-1}, respectively, which are higher than the B3P86 calculated Cu–O stretching frequency of 602 cm^{-1} in CuO ($^2\Pi$) species. For the $^2B_1$ state of $(O_2)CuO$ (I), a Cu–O stretching vibrational frequency is 689 cm^{-1}. B3P86 calculations show that these Cu–O stretching bands in the region of 600 cm^{-1} are very weak. This is in agreement with the fact that no Cu–O vibrational band was observed for the low-lying states in the anion photoelectron spectroscopic experiment [9]. Presumably, the only observed band of 660(90) cm^{-1} in the excited state named D at 4.34 eV in reference [9] should be related to the Cu–O stretching in this excited state, even though our calculations cannot assign the nature of the excited state D.

Among the anionic isomers containing an O_3 subunit, the most stable $^1A'$ state of the top-on coordination $Cu(O_3)^-$ (V) has a Cu–(O_3) stretching frequency of 299 cm^{-1}, while the Cu–(O_3) stretching band is at 367 cm^{-1} for the stable $^3B_2$ state of the side-on coordination $Cu(O_3)^-$ (III), showing that the interaction of Cu with O_3 in the side-on structure should be stronger than that in the top-on isomer. For the neutral isomers with the O_3 bonded to Cu, the $^2B_1$ and $^2B_2$ states have Cu–(O_3) stretching frequencies of 338 and 344 cm^{-1}, respectively. From intensities listed in Table I, it can be seen that all these bands accounting for Cu–(O_3) stretching are very weak, while strong bands in higher frequency region are derived from O_3 bonded to Cu.

Table II collects electron binding energies at the B3P86 and B3LYP levels of theory. The B3P86 electron binding energies are larger than B3LYP values by about 0.4 eV. To test the reliability of these B3P86 and B3LYP relative energies, we performed CCSD(T)//B3P86 calculations on the $^3A''$ (II) state of CuO_3^- and the $^4A_1$ (I) and $^4A''$ (II) states of CuO_3. The energy difference between the $^3A''$ (II) state of CuO_3^- and the $^4A_1$ (I) state of CuO_3 at the CCSD(T)//B3P86 level is 2.85 eV in perfect agreement with the B3LYP value (2.86 eV) and about 0.5 eV smaller than the B3P86 result (3.32 eV). On the other hand, the energy difference between the $^3A''$ (II) state of CuO_3^- and the $^4A''$ (II) state of CuO_3 is 2.81 eV at the CCSD(T)//BP86 level, a value closer to the B3LYP result (3.00 eV) than to the B3P86 value (3.48 eV). These results show that the B3LYP electron binding energies are more reliable than those obtained with the B3P86 method. From the B3LYP values of Table II, one can see that the adiabatic (vertical) ionization potentials of the most stable $^3A''$ (II) state and the next most stable $^1A_1$ (I) state of CuO_3^- species

are predicted to be 3.00 (3.25) and 3.13 (3.38) eV, respectively, which are comparable to the observed 3.19 and 3.39 eV [9]. Thus, the most stable $^3A''$ (II) state and the next most stable $^1A_1$ (I) state of CuO_3^- may be tentatively assigned to the ground state and the first excited state of CuO_3^- observed in the experiment [9], respectively. We must note that in the original work, the 3.19-eV structure was tentatively assigned to a side-on structure (I) [9]. Results from our calculations does not rule out this possibility although they suggest that the 3.19 eV structure is an end-on structure (II). The electron binding energies of the anion isomers containing an O_3 subunit bound to Cu are in the region of 1.8 eV at the B3LYP and B3P86 levels, close to the observed value of 1.78 eV for CuO^- [9].

The bonding between O_2 and CuO in CuO_3^- should be substantial since the ionization potential of CuO_3^- (3.19 eV) is increased significantly compared to CuO^- (1.78 eV) [9]. This point is confirmed by the B3LYP and B3P86 dissociation energies of stable CuO_3^- species displayed in Table III. These calculated dissociation energies at the B3LYP and B3P86 levels show that the anionic species formed by O_2 bound to CuO and O_3 bonded to Cu are more stable than their corresponding dissociation limits. Compared to the B3LYP calculation, B3P86 calculations predict slightly higher dissociation energies. This notwithstanding, the energies required for the dissociation channels considered in Table III are not extremely high. Furthermore, there exist vibrational modes correlating to dissociation processes (O_2)–CuO and (O_3)–Cu for these stable CuO_3^- isomers. Thus, photodissociation of these CuO_3^- species leading to products of $Cu^- + O_3$ and $CuO^- + O_2$ seem to be possible, even though these processes need more energy than those dissociating into $Cu + O_3^-$ and $CuO + O_2^-$. This is in accordance with the fact that the photoelectron features of Cu^- and CuO^- exist along with the photoelectron spectra of CuO_3^- [9].

Finally, it is interesting to discuss the chemical bonding in CuO_3^- species. We have carried out a natural population and a NBO analysis for selected states in order to get further insight into the bonding features of CuO_3^- species. From the results of Table IV we note that large changes in the *d* population of Cu occur, compared to the ground state of Cu ($d^{10}s^1$), except for the $^1A'$ state of the top-on $Cu(O_3^-)$ (V) isomer, showing that the *d* electrons of Cu have a significant contribution to chemical bonding and suggesting a partial covalent character of the bond. The occupancies and compositions of the NBO for the $^1A_1$ $(O_2)CuO^-$ (I) and the $^3A''$ $OOCuO^-$ (II) show that the *d* orbitals of Cu contribute to the Cu–O bonding in the CuO subunit and does not participate in molecular bonding between the subunit O_2 and CuO. The NBO charges on the O_2 and CuO subunits are −0.98 and −0.02 for the $^1A_1$ $(O_2)CuO^-$ (I), and −0.85 and −0.15 for the $^3A''$ $OOCuO^-$ (II). Thus, the molecular bonding in both states can be viewed as the result of an O_2^-–CuO donor–acceptor interaction, where O_2^- behaves as a donor and CuO behaves as an acceptor. In the $^1A_1$ $(O_2)CuO^-$ (I) complex, the donation from an occupied π orbital of O_2^- to the 4*s* orbital of Cu^+ in CuO and backdonation from occupied 3*d* orbitals of copper to the π^* orbitals of O_2^- results in a significant lengthening of the O–O bond, which is 1.382 Å in $^1A_1$ $(O_2)CuO^-$ (I) as compared to 1.334 Å in isolated O_2^- at the B3P86 level of theory. The net charge transfer from O_2^- to CuO is 0.02 electrons only. In the $^3A''$ $OOCuO^-$ (II) system, the main interaction, which is a donation from a π^* orbital of O_2^- to the 4*s* orbital of Cu^+ in CuO, results in a larger charge transfer (0.15 electrons) and a slightly shorter O–O distance of 1.330 Å as compared again to the O–O distance of 1.334 Å in isolated O_2^-.

TABLE IV

Natural population analysis of the B3LYP wave function for selected states, showing natural charge *q* (in a.u.) and effective valence shell natural electron configuration (NEC).

State	Atom	*q*	NEC
$^1A_1$ $(O_2)CuO^-$ (I)	Cu	1.135	$4s^{0.44}\ 3d^{9.36}$
	O_1	−1.154	$2s^{1.95}\ 2p^{5.19}$
	O_2	−0.490	$2s^{1.85}\ 2p^{4.61}$
$^3A''$ $OOCuO^-$ (II)	Cu	0.756	$4s^{0.59}\ 3d^{9.62}$
	O_1	−0.902	$2s^{1.96}\ 2p^{4.94}$
	O_2	−0.491	$2s^{1.81}\ 2p^{4.65}$
	O_3	−0.363	$2s^{1.84}\ 2p^{4.49}$
$^3B_2$ $Cu(O_3)^-$ (III)	Cu	0.370	$4s^{1.02}\ 3d^{9.43}$
	O_1	−0.161	$2s^{1.79}\ 2p^{4.33}$
	O_2	−0.604	$2s^{1.89}\ 2p^{4.68}$
$^1A'$ $Cu(O_3)^-$ (V)	Cu	0.493	$4s^{0.51}\ 3d^{9.90}$
	O_1	−0.166	$2s^{1.76}\ 2p^{4.36}$
	O_2	−0.664	$2s^{1.89}\ 2p^{4.75}$
$^4A_1$ $(O_2)CuO$ (I)	Cu	1.046	$4s^{0.41}\ 3d^{9.50}$
	O_1	−0.619	$2s^{1.96}\ 2p^{4.64}$
	O_2	−0.214	$2s^{1.83}\ 2p^{4.35}$

Conclusions

The molecular structures and harmonic vibrational frequencies of CuO_3^- and CuO_3 species have been reported at the DFT level. The electron binding energies and dissociation energies for CuO_3^- isomers have been predicted by hybrid DFT methods. The present calculations show that two types of stable isomers exist for CuO_3 systems. One is composed of O_2 bound to CuO in side-on and end-on coordination and the other contains an O_3 subunit. The isomers formed by O_2 bonded to CuO are lower in energy than those containing an O_3 subunit.

ACKNOWLEDGMENTS

This work has been supported by the Spanish DGES Project No. PB98-0457-C02-01 and the China NSF Project No. 29773036. One of us (Z.C.) gratefully acknowledges the Catalan Comissionat per a Universitats i Recerca for a fellowship to work in Girona.

References

1. Cox, P. A. Transition Metal Oxides; Oxford: New York, 1995.
2. Halfen, J. A.; Mahapatra, S.; Wilkinson, E. E.; Kaderli, S.; Young, Jr., V. G.; Que, Jr., L.; Zuberbuhler, A. D.; Tolman, W. B. Science 1996, 271, 1397.
3. Langhoff, S. R.; Bauschlicher, C. W. Chem Phys Lett 1986, 124, 241.
4. Merer, A. J. Annu Rev Phys Chem 1989, 40, 407.
5. Brown, C. E.; Mitchell, S. A.; Hachett, P. A. J Phys Chem 1991, 95, 1062.
6. Ozin, G. A.; Mitchell, S. A.; Garcia-Prieto, J. J Am Chem Soc 1983, 105, 6399.
7. Bauschlicher, Jr., C. W.; Langhoff, S.; Partridge, H.; Sodupe, M. J Phys Chem 1993, 97, 856.
8. Hrusak, J.; Koch, W.; Schwarz, H. J Chem Phys 1994, 101, 3898.
9. Wu, H.; Desai, S. R.; Wang, L.-S. J Phys Chem A 1997, 101, 2103.
10. Jursic, B. S. Int J Quantum Chem 1997, 61, 93.
11. (a) Barone, V.; Adamo, C. Int J Quantum Chem 1997, 61, 443; (b) Barone, V.; Adamo, C. J Phys Chem 1996, 100, 2094.
12. Bauschlicher, C. W.; Langhoff, S. R. Spectrochim Acta A 1997, 53, 1225.
13. Andrews, L.; Chertihin, G. V.; Thompson, C. A.; Dillon, J.; Byrne, S.; Bauschlicher, C. W. J Phys Chem 1996, 100, 10088.
14. Andrews, L.; Citra, A.; Chertilin, G. V.; Bare, W. D.; Neurock, M. J. J Phys Chem A 1998, 102, 2561.
15. Cotton, F. A.; Feng, X. J. J Am Chem Soc 1998, 120, 3387.
16. (a) Wagener, T.; Frenking, G. Inorg Chem 1998, 37, 1805; (b) Torrent, M.; Solà, M.; Frenking, G. Chem Rev 2000, 100, 439; (c) Torrent, M.; Solà, M.; Frenking, G. Organometallics 1999, 18, 2801.
17. (a) Davidson, E. R. Chem Phys Lett 1998, 284, 301; (b) Torrent, M.; Gili, P.; Duran, M.; Solà, M. J Chem Phys 1996, 106, 9499.
18. Becke, A. D. J Chem Phys 1993, 98, 5648.
19. Perdew, J. P. Phys Rev B 1986, 33, 8822.
20. Lee, C.; Yang, W.; Parr, R. G. Phys Rev B 1988, 37, 785.
21. Frisch, M. J.; Trucks, G. W; Schlegel, H. B.; Gill, P. M. W.; Johnson, B. G.; Robb, M. A.; Cheesman, J. R.; Keith, T.; Petersson, G. A.; Montgomery, J. A.; Raghavachari, K.; Al-Laham, M. A.; Zakrzewski, V. G.; Ortiz, J. V.; Foresman, J. B.; Peng, C. Y.; Ayala, P. Y.; Chen, W.; Wong, M. W.; Andres, J. L.; Replogle, E. S.; Gomperts, R.; Martin, R. L.; Fox, D. J.; Binkley, J. S.; Defrees, D. J.; Baker, J.; Stewart, J. J. P.; Head-Gordon, M.; Gonzalez, C.; Pople, J. A. Gaussian 94, Revision A.1; Gaussian: Pittsburgh, 1995.
22. (a) Barlett, R. G.; Purvis, G. D. Int J Quantum Chem 1978, 14, 516; (b) Scuseria, G. E.; Schaeffer, III, H. F. J Chem Phys 1989, 90, 3700.
23. Glendening, E. D.; Reed, A. E.; Carpenter, J. E.; Weinhold, F. NBO Version 3.1.
24. Wachters, A. J. H. J Chem Phys 1970, 52, 1033.
25. Hay, P. J. J Chem Phys 1977, 66, 4377.
26. Raghavachari, K.; Trucks, G. W. J Chem Phys 1989, 91, 1062.